

Echoes from the Black Hole Microstructure

Alexandru Dima

Sapienza University of Rome & INFN Roma 1

@ XVIII BHs Workshop 2025, IST, Lisbon



SAPIENZA
UNIVERSITÀ DI ROMA



Summary

1. **What?** Novel gravitational solitons
2. **Why?** BH mimickers / BH microstate “toy model”
3. **How?** Time domain numerical evolution
4. Conclusion and future prospects

Based on:

AD, M. Melis, P. Pani, *PRD* 110 (2024) 8, 084067, [arXiv:2406.19327](https://arxiv.org/abs/2406.19327)

AD, M. Melis, P. Pani, *PRD* 111 (2025) 10, 104001, [arXiv:2502.04444](https://arxiv.org/abs/2502.04444)

AD, P. Heidmann, M. Melis, P. Pani, G. Patashuri, *PRD* 112 (2025), 124056, [arXiv:2509.18245](https://arxiv.org/abs/2509.18245)

What?

New viable mimickers

Topological solitons in 5D Einstein-Maxwell:

$$\mathcal{S}_{EM} = \frac{1}{16\pi G_5} \int d^5x \sqrt{-g} \left(R_5 - \frac{1}{4} F_{AB} F^{AB} \right)$$

$$ds^2 = -f_S(r)dt^2 + f_B(r)dy^2 + \frac{1}{h(r)}dr^2 + r^2 d\Omega_2^2 \quad F = P \sin \theta \, d\theta \wedge d\phi$$

$$f_B(r) = 1 - \frac{r_B}{r}, \quad f_S(r) = 1 - \frac{r_S}{r}, \quad h(r) = f_B(r)f_S(r), \quad P = \pm \kappa_5^{-1} \sqrt{\frac{3}{2} r_B r_S}$$

Bah & Heidmann (2020; 2021)

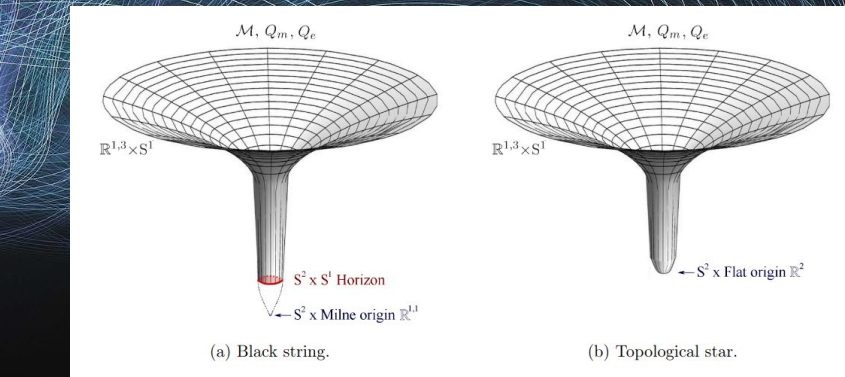
W-solitons in 5D EM + Chern-Simons:

$$\mathcal{S}_{EMCS} = \frac{1}{16\pi G_5} \int d^5x \sqrt{-g} \left(R_5 - \frac{1}{4} F_{AB} F^{AB} - \frac{\lambda}{12} \epsilon^{ABCDE} F_{AB} F_{CD} A_E \right)$$

$$ds_W^2|_{Q=0} = - \left(1 - \frac{2M}{r} \right) dt^2 + \frac{r-2M}{r-4M} dr^2 + \frac{r(r-4M)}{(r-2M)^2} d\psi^2 + r(r-2M)(d\theta^2 + \sin^2 \theta \, d\phi^2)$$

$$A = \frac{2M}{r-2M} d\psi,$$

Chakraborty & Heidmann (2025)



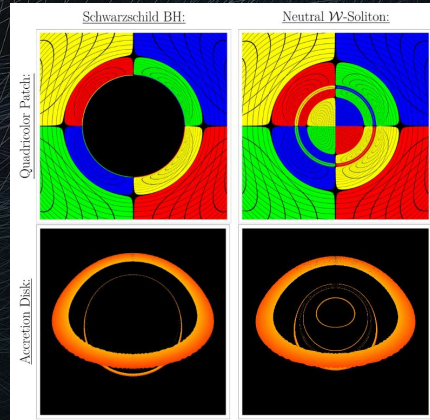
(a) Black string.

(b) Topological star.

Bah & Heidmann (2021)

- asymptotically $\mathbb{R}^{1,3} \times S^1$
- conserved charges as BH
- horizon \rightarrow smooth cap
- no singularity
- ultracompact

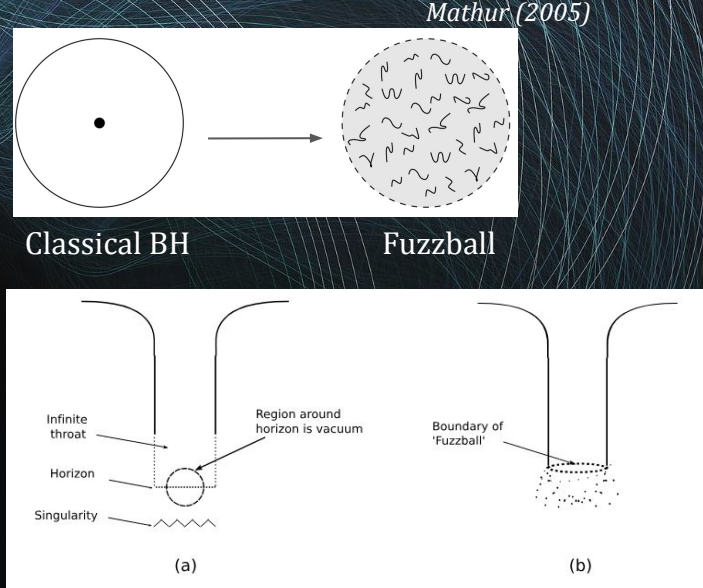
Dima et al. (2025)



Why?

Pheno & UV motivation

- Consistent **BH mimickers**:
 - ultracompact, regular and horizonless
 - solutions of a consistent theory
 - BH-like compactness
 - 1 or 2 lightrings
- “Toy” models of coherent **fuzzball microstates**:
 - smooth horizon-scale structure
 - extra compact dimensions + non-trivial topology
 - Non-extremal BH microstates
 - Reduced dimensionality
 - Spherical symmetry

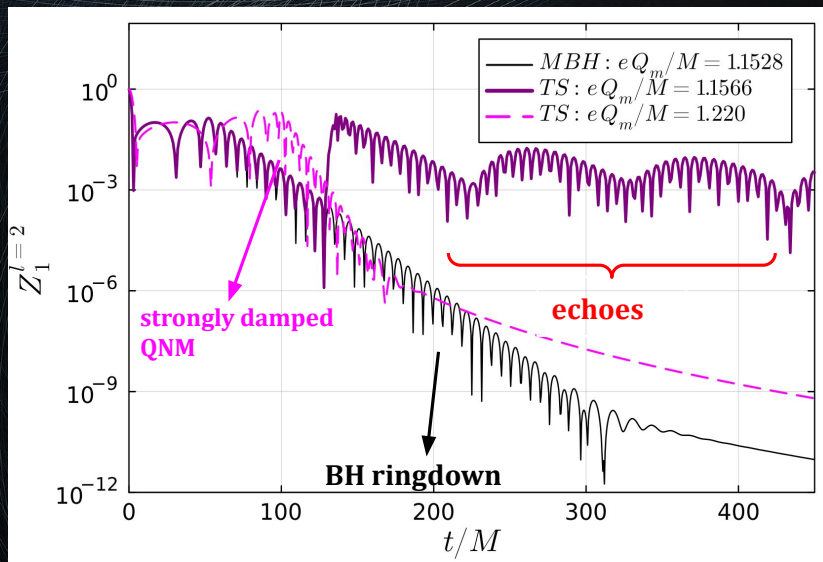


Mathur (2008)

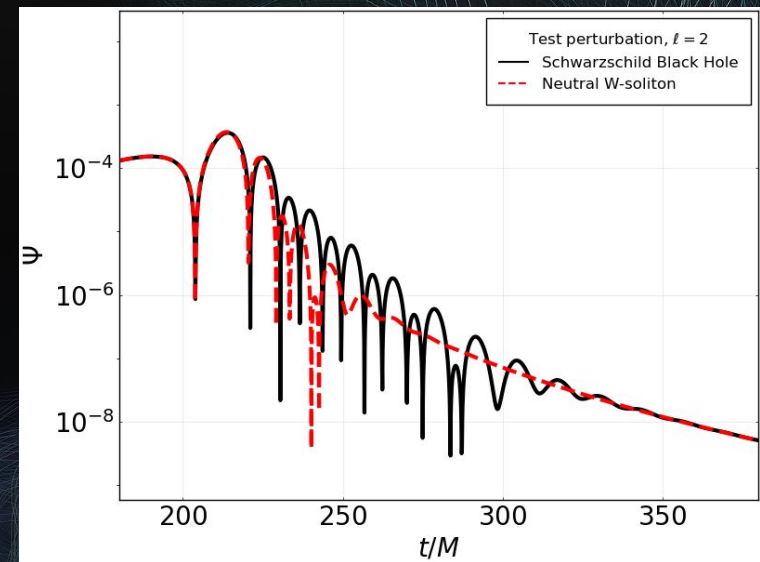
How?

Time domain simulations

Gravitational perturbations of Topological Solitons vs Magnetized BH



Test perturbations of W-soliton vs Schwarzschild BH



Conclusions

Results:

- Geodesics and Lensing on W-soliton spacetime
- Linear stability of topological solitons
- Linear spectrum: QNMs & Echoes

What's next?

- Full linear stability analysis of W-solitons*
- Linear perturbations of rotating/axisymmetric solitons
- 1+1 nonlinear evolution of topological solitons
(AD, F. Corelli, P. Pani, in preparation)
- Full NR 3+1 simulations of isolated + binary soliton systems
- Numerical waveform model of coalescing microstate geometries



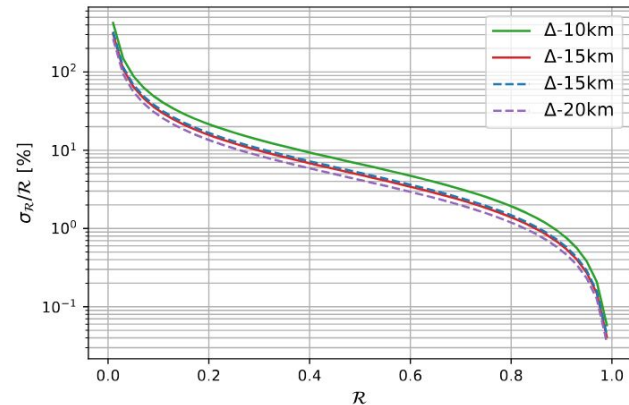
Backup slides

Black Hole mimickers: a target for GW detectors

- **Black Hole mimickers:** ultra compact, **regular** and **horizonless** objects
Bambi et al. (2025)
- Most are **bottom-up** models (boson stars, gravastars, wormholes)

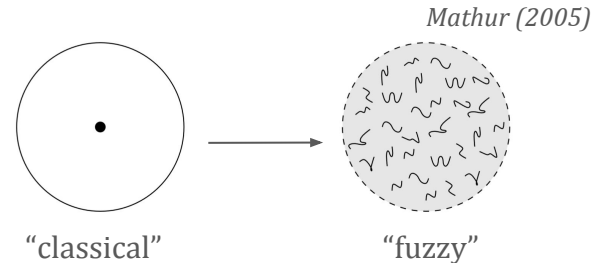
- Possible signatures:
 - Non-trivial **Tidal deformability**
 - Anomalous **spin-induced quadrupole moment**
 - **Echoes** in the ringdown

Cardoso, Franzin, Pani (2016); Cardoso & Pani (2019)



- 2G detectors are limited: SNR $\sim 0(100)$ required for echoes detection
Testa & Pani (2017); Maggio et al. (2019); Abbott et al. (2021)
- ET (and other 3G detectors) could make a difference!
Maggiore et al. (2020); Branchesi et al. (2023)

The fuzzball paradigm



- String Theory's **fuzzballs**: ensembles of **many**, **smooth** and **horizonless** microstates
- Microstate geometries: **BH asymptotics, horizon-scale structure**
Lunin & Mathur (2002); Mathur (2005, 2008); Meyerson (2020)
- supported via **higher dimensions and non-trivial topology** *Gibbons & Warner (2014)*
- Known microstates: **supersymmetric (or extremal)**, many charges, complex geometries
- Few phenomenological studies
Bianchi et al. (2018a, 2018b); Bena et al. (2018, 2019); Ikeda et al. (2021).
Bena, Warner (2008, 2013); Bena et al., (2011); Bena, Shigemori, Warner (2014); Bianchi et al., (2017); ...

Topological Stars

$$M = \frac{2\pi}{\kappa_4^2} (2r_S + r_B), \quad Q_m = \frac{1}{\kappa_4} \sqrt{\frac{3}{2} r_S r_B}$$

- **1st kind TS**: $\frac{3}{2}r_S \leq r_B \leq 2r_S$

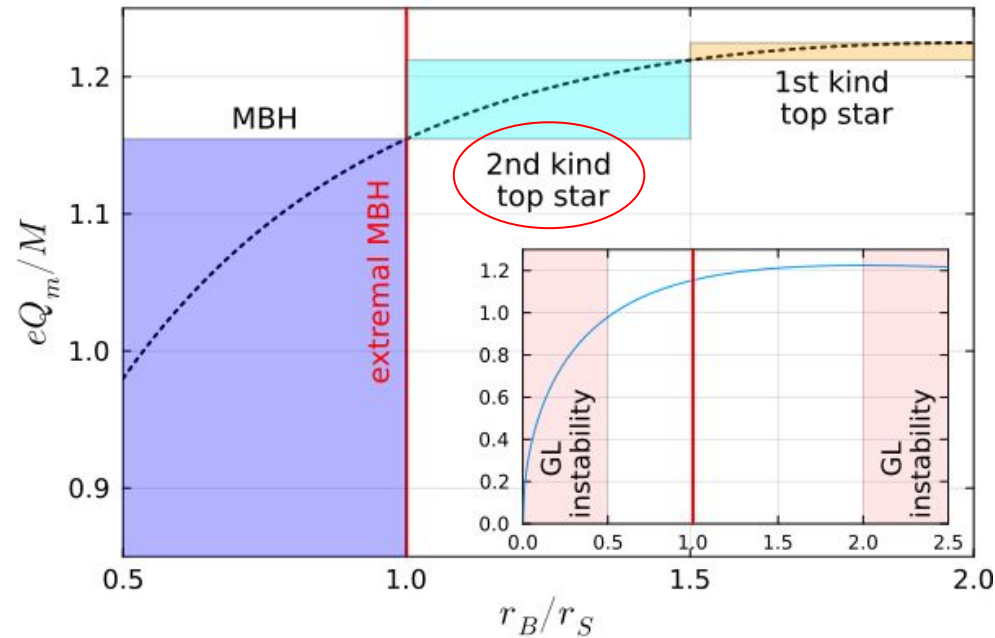
$$r_{(ph)} = r_B \\ \text{(unstable)}$$

- **2nd kind TS**: $r_S < r_B < \frac{3}{2}r_S$

$$r_{(ph)} = \frac{3}{2}r_S, \quad r_{(ph)} = r_B \\ \text{(stable)} \quad \text{(unstable)}$$

Gregory-Laflamme instability:

$$r_B < \frac{1}{2}r_S, \quad r_B > 2r_S$$



Regge-Wheeler-Zerilli perturbation scheme (5D)

Type-I

axial gravitational + polar EM ($l \geq 1$)

$$h_{AB}^{\text{odd}} = \sum_{l,m} \begin{pmatrix} 0 & 0 & 0 & -h_0(t, y, r) / \sin \theta \partial_\phi & h_0(t, y, r) \sin \theta \partial_\theta \\ 0 & 0 & 0 & -h_2(t, y, r) / \sin \theta \partial_\phi & h_2(t, y, r) \sin \theta \partial_\theta \\ 0 & 0 & 0 & -h_1(t, y, r) / \sin \theta \partial_\phi & h_1(t, y, r) \sin \theta \partial_\theta \\ -h_0(t, y, r) / \sin \theta \partial_\phi & -h_2(t, y, r) / \sin \theta \partial_\phi & -h_1(t, y, r) / \sin \theta \partial_\phi & 0 & 0 \\ h_0(t, y, r) \sin \theta \partial_\theta & h_2(t, y, r) \sin \theta \partial_\theta & h_1(t, y, r) \sin \theta \partial_\theta & 0 & 0 \end{pmatrix} Y_{lm}(\theta, \phi)$$

$$f_{AB}^{\text{even}} = \sum_{l,m} \begin{pmatrix} 0 & f_{ty}^+(t, r) & f_{tr}^+(t, r) & f_{t\theta}^+(t, r) \partial_\theta & f_{t\phi}^+(t, r) \partial_\phi \\ -f_{ty}^+(t, r) & 0 & f_{yr}^+(t, r) & f_{y\theta}^+(t, r) \partial_\theta & f_{y\phi}^+(t, r) \partial_\phi \\ -f_{tr}^+(t, r) & -f_{yr}^+(t, r) & 0 & f_{r\theta}^+(t, r) \partial_\theta & f_{r\phi}^+(t, r) \partial_\phi \\ -f_{t\theta}^+(t, r) \partial_\theta & -f_{y\theta}^+(t, r) \partial_\theta & -f_{r\theta}^+(t, r) \partial_\theta & 0 & 0 \\ -f_{t\phi}^+(t, r) \partial_\phi & -f_{y\phi}^+(t, r) \partial_\phi & -f_{r\phi}^+(t, r) \partial_\phi & 0 & 0 \end{pmatrix} Y_{lm}(\theta, \phi)$$

Type-II

polar gravitational + polar scalar + axial EM ($l \geq 0$)

$$h_{AB}^{\text{even}} = \sum_{l,m} \begin{pmatrix} f_S H_0(t, y, r) & H_4(t, y, r) & H_1(t, y, r) & 0 & 0 \\ H_4(t, y, r) & f_B H_3(t, y, r) & H_5(t, y, r) & 0 & 0 \\ H_1(t, y, r) & H_5(t, y, r) & (f_S f_B)^{-1} H_2(t, y, r) & 0 & 0 \\ 0 & 0 & 0 & r^2 K(t, y, r) & 0 \\ 0 & 0 & 0 & 0 & r^2 \sin \theta^2 K(t, y, r) \end{pmatrix} Y_{lm}(\theta, \phi)$$

$$f_{AB}^{\text{odd}} = \sum_{l,m} \begin{pmatrix} 0 & 0 & 0 & f_{t\theta}^-(t, r) / \sin \theta \partial_\phi & -f_{t\phi}^-(t, r) \sin \theta \partial_\theta \\ 0 & 0 & 0 & f_{y\theta}^-(t, r) / \sin \theta \partial_\phi & -f_{y\phi}^-(t, r) \sin \theta \partial_\theta \\ 0 & 0 & 0 & f_{r\theta}^-(t, r) / \sin \theta \partial_\phi & -f_{r\phi}^-(t, r) \sin \theta \partial_\theta \\ -f_{t\theta}^-(t, r) / \sin \theta \partial_\phi & -f_{y\theta}^-(t, r) / \sin \theta \partial_\phi & -f_{r\theta}^-(t, r) / \sin \theta \partial_\phi & 0 & \Lambda f_{\theta\phi}^-(t, r) \sin \theta \\ f_{t\theta}^-(t, r) \sin \theta \partial_\theta & f_{y\theta}^-(t, r) \sin \theta \partial_\theta & f_{r\theta}^-(t, r) \sin \theta \partial_\theta & -\Lambda f_{\theta\phi}^-(t, r) \sin \theta & 0 \end{pmatrix} Y_{lm}(\theta, \phi)$$

Perturbed equations in canonical form:

Reduction to 4D,

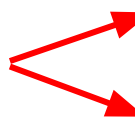
$$\sigma = 0$$



$$\left[\frac{d^2}{dt^2} - \frac{d^2}{d\rho^2} + V_{\text{eff}} \right] \Psi(t, \rho) = 0$$

F-domain: matrix-based QNM solver

T-domain: 1+1 pde solver



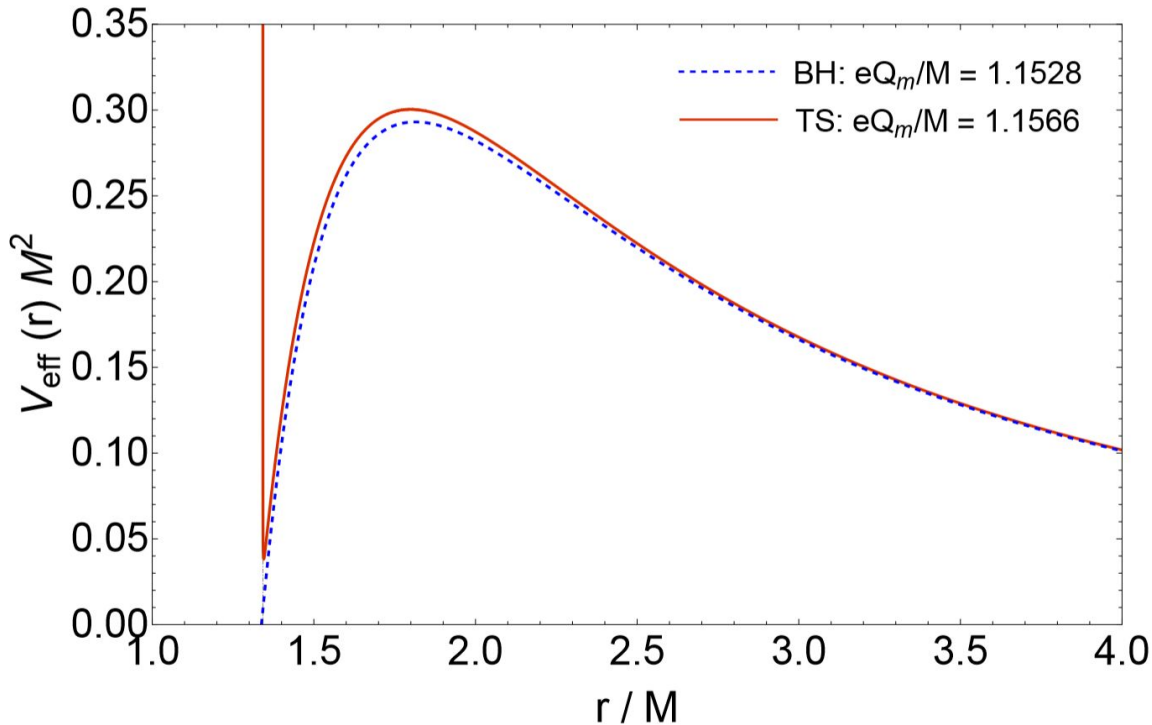
Where do the echoes come from?

Near-extremal MBH:

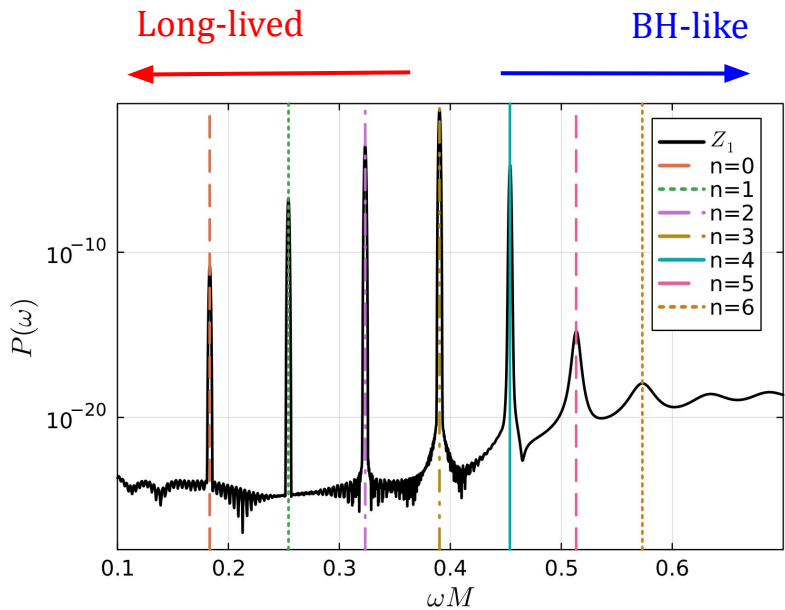
- Effective potential barrier
- Potential vanishes asymptotically

2nd kind Top Star:

- Same BH asymptotics at large distances
- “Small” corrections at the potential peak
- Reflective “surface”!
- Potential well leads to **trapped modes!**



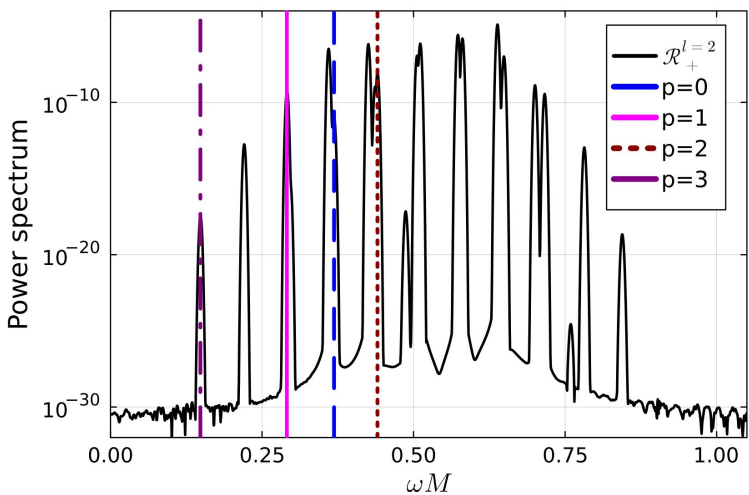
Type-I QNMs: QNM Spectrum



		Magnetized BH	TS, second kind	TS, first kind
$n = 0$	f-domain	$0.489568 - i 7.972 \times 10^{-2}$	$0.183217 - i 4.674 \times 10^{-10}$	$0.644348 - i 0.1551$
	t-domain	$0.489600 - i 7.978 \times 10^{-2}$	$0.183219 - i 3.349 \times 10^{-10}$	$0.643938 - i 0.1665$
$n = 1$	f-domain	-	$0.254071 - i 6.001 \times 10^{-8}$	-
	t-domain	-	$0.254084 - i 6.008 \times 10^{-8}$	-
$n = 2$	f-domain	-	$0.323219 - i 2.615 \times 10^{-6}$	-
	t-domain	-	$0.323263 - i 2.622 \times 10^{-6}$	-
$n = 3$	f-domain	-	$0.390169 - i 6.116 \times 10^{-5}$	-
	t-domain	-	$0.390256 - i 6.142 \times 10^{-5}$	-
$n = 4$	f-domain	-	$0.453786 - i 8.348 \times 10^{-4}$	-
	t-domain	-	$0.453832 - i 8.340 \times 10^{-4}$	-
$n = 5$	f-domain	-	$0.513765 - i 5.463 \times 10^{-3}$	-
	t-domain	-	$0.513375 - i 2.754 \times 10^{-3}$	-
$n = 6$	f-domain	-	$0.574947 - i 1.658 \times 10^{-2}$	-
	t-domain	-	$0.572869 - i 1.140 \times 10^{-2}$	-

Type-II QNMs: QNM Spectrum

Gravity-induced perturbations ($l=2$)

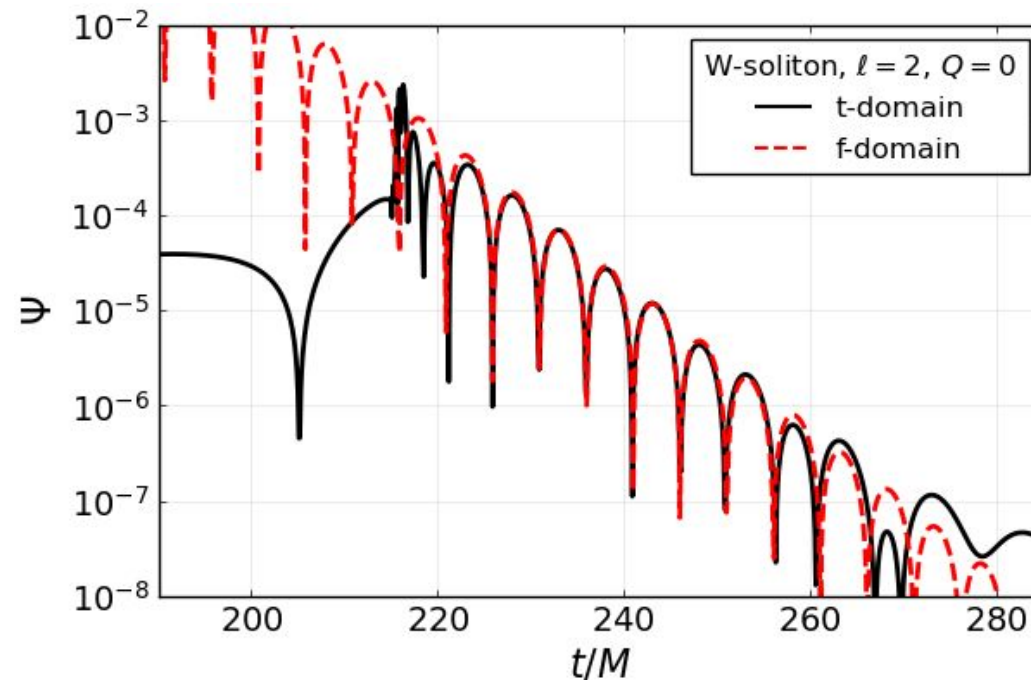


$rs/r_B =$	7/10	9/10	19/20	99/100	
$l = 1$	$p = 0$ f-domain t-domain	$0.725735 - i9.739 \times 10^{-2}$ $0.725753 - i9.735 \times 10^{-2}$	$0.594653 - i3.979 \times 10^{-3}$ $0.594636 - i3.978 \times 10^{-3}$	$0.463193 - i2.163 \times 10^{-5}$ $0.463183 - i2.160 \times 10^{-5}$	$0.221521 - i1.967 \times 10^{-11}$ $0.221438 - i2.110 \times 10^{-11}$
	$p = 1$ f-domain t-domain	-	$0.543775 - i4.233 \times 10^{-2}$ $0.549296 - i3.719 \times 10^{-2}$	$0.581303 - i4.013 \times 10^{-3}$ $0.581265 - i4.006 \times 10^{-3}$	$0.293106 - i4.147 \times 10^{-9}$ $0.292507 - i4.089 \times 10^{-9}$
	$p = 2$ f-domain t-domain	-	$0.708010 - i6.095 \times 10^{-2}$ $0.709243 - i5.997 \times 10^{-2}$	$0.441270 - i3.926 \times 10^{-3}$ $0.441245 - i3.910 \times 10^{-3}$	$0.220050 - i1.896 \times 10^{-7}$ $0.220049 - i1.875 \times 10^{-7}$
	$p = 3$ f-domain t-domain	-	-	$0.681979 - i3.779 \times 10^{-2}$ $0.682161 - i3.173 \times 10^{-2}$	$0.362912 - i2.424 \times 10^{-7}$ $0.362168 - i2.329 \times 10^{-7}$
$rs/r_B =$	7/10	9/10	19/20	99/100	
$p = 0$ f-domain t-domain	$0.569028 - i4.955 \times 10^{-2}$ $0.569024 - i4.981 \times 10^{-2}$	$0.834579 - i1.619 \times 10^{-4}$ $0.834486 - i1.865 \times 10^{-4}$	$0.630961 - i2.895 \times 10^{-8}$ $0.630844 - i3.245 \times 10^{-8}$	$0.368629 - i3.221 \times 10^{-14}$ $0.368733 - i(*)$	
$l = 2$	$p = 1$ f-domain t-domain	$1.085261 - i7.599 \times 10^{-2}$ $1.085059 - i7.557 \times 10^{-2}$	$0.422771 - i6.856 \times 10^{-4}$ $0.424131 - i7.271 \times 10^{-4}$	$0.317783 - i5.510 \times 10^{-6}$ $0.317827 - i5.551 \times 10^{-6}$	$0.295274 - i3.206 \times 10^{-12}$ $0.295660 - i(*)$
	$p = 2$ f-domain t-domain	-	$0.782183 - i1.144 \times 10^{-2}$ $0.782285 - i1.146 \times 10^{-2}$	$0.764893 - i2.534 \times 10^{-5}$ $0.765489 - i3.821 \times 10^{-5}$	$0.439992 - i3.944 \times 10^{-12}$ $0.440391 - i(*)$
	$p = 3$ f-domain t-domain	-	$0.960878 - i1.792 \times 10^{-2}$ $0.961672 - i1.825 \times 10^{-2}$	$0.616095 - i4.239 \times 10^{-5}$ $0.616099 - i4.103 \times 10^{-5}$	$0.148446 - i6.337 \times 10^{-11}$ $0.148477 - i6.262 \times 10^{-11}$

TABLE II. Same as in Table I but for TSs with $eQ_m/M \approx \{1.208, 1.174, 1.164, 1.157\}$ (equivalently, $rs/r_B = \{0.70, 0.90, 0.95, 0.99\}$). The asterisk indicates QNMs with a characteristic damping time that is too large for the spectral analysis to retrieve an accurate fit thereof.

W-soliton: t-domain vs f-domain

Neutral soliton
test field
ringdown



W-soliton: test field perturbation

Charged W-soliton vs charged black string, test field response:

